Association Between Alterations of the Choriocapillaris Microcirculation and Visual Function and Cone Photoreceptors in Patients With Diabetes

Tomoko Ro-Mase,[1] Satoshi Ishiko,[2] Tsuneaki Omae,[1] Akihiro Ishibazawa,[1] Akito Shimouchi,[1] and Akitoshi Yoshida[1]

[1]Department of Ophthalmology, Asahikawa Medical University, Asahikawa, Japan
[2]Department of Medicine and Engineering Combined Research Institute, Asahikawa Medical University, Asahikawa, Japan

Correspondence: Satoshi Ishiko, Department of Medicine and Engineering Combined Research Institute, Asahikawa Medical University, Midorigaoka Higashi 2-1-1-1, Asahikawa 078-8510, Japan; ishiko@asahikawa-med.ac.jp.

Received: December 13, 2019
Accepted: May 5, 2020
Published: June 3, 2020

Citation: Ro-Mase T, Ishiko S, Omae T, Ishibazawa A, Shimouchi A, Yoshida A. Association between alterations of the choriocapillaris microcirculation and visual function and cone photoreceptors in patients with diabetes. *Invest Ophthalmol Vis Sci.* 2020;61(6):1. https://doi.org/10.1167/iovs.61.6.1

Purpose. The purpose of this study was to investigate the association between the choriocapillaris microcirculation and the visual function and cone photoreceptor structure in patients with diabetes.

Methods. Thirteen control subjects and 26 patients with type 2 diabetes were recruited. The patients with diabetes were divided into three groups based on the grade of diabetic retinopathy (DR). The retinal sensitivity (RS) was evaluated using microperimetry. Cone photoreceptor mosaics were imaged using an adaptive optics retinal camera, and the cone heterogeneity packing index (HPi) was calculated. Optical coherence tomography angiography (OCTA) images of the choriocapillaris were obtained using spectral-domain OCTA, and the area of flow deficit (FD) was evaluated. All parameters were evaluated in the foveal and parafoveal areas.

Results. The study included four patients with diabetes without retinopathy, 12 patients with nonproliferative diabetic retinopathy (NPDR), and 10 patients with proliferative diabetic retinopathy (PDR). The foveal and parafoveal FDs were correlated significantly (fovea, $r = -0.58$; $P = 0.046$ and $r = -0.82$; $P = 0.003$; parafovea, $r = -0.59$; $P = 0.044$ and $r = -0.72$; and $P = 0.019$, respectively) with the RS in patients with NPDR and PDR, but not in control and no diabetic retinopathy (NDR) groups. There were no differences in the foveal HPi among the groups.

Conclusions. Impaired choriocapillaris microcirculation is associated with impaired visual function but not cone photoreceptor integrity in eyes with DR.

Keywords: diabetic retinopathy, optical coherence tomography angiography, choriocapillaris, visual function, cone photoreceptors

Diabetic retinopathy (DR), clinically defined as a microangiopathy in the retina, is a leading cause of visual loss.[1] Microangiopathy in diabetic eyes affects two microcirculatory systems that supply oxygen and nutrients to the neural retinal tissue: the retinal circulation, which supplies the inner retinal layer and about 10% to 15% of the outer retina,[2] and the choroidal circulation, which mainly covers the outer retinal layer, including the photoreceptor layer through the choriocapillaris.[3] In addition to the traditional idea that retinal circulatory disruption is the main culprit in visual functional loss, accumulating evidence suggests that the choroidal circulation also may be affected in diabetic eyes and contribute to the outer retinal damage. Histologic studies have shown choriocapillaris abnormalities, such as vessel dropout, ischemia, and aneurysms, in diabetic eyes.[4] In addition, in eyes with DR, disruption of the choroidal circulation is accompanied by loss of the ellipsoid zone,[5] which is thought to represent the mitochondria in the photoreceptors.[6] Therefore, impaired choroidal microcirculation also may affect the photoreceptor structures/functions in diabetic eyes. Taken together, choroidal circulatory disruption likely causes visual functional loss.[7,8] However, the association between the choroidal circulatory disturbances and the photoreceptor structure has not been investigated quantitatively, especially in diabetic eyes.

Thus far, no studies have used a combination of high-resolution imaging modalities and high-spatial resolution functional studies to investigate the association between the choroidal circulation and visual function, although more attention is starting to be paid to the choroidal circulation. Optical coherence tomography angiography (OCTA), for example, shows the blood flow and density in the retina and choriocapillaris quantitatively. Using OCTA, clinical studies have reported structural alterations of the choroidal vasculature in a quantitative manner in eyes with DR[9–13] using an area of flow deficit (FD), which is an index of capillary loss in the choriocapillaris layer,[14–16] or a similar index.[5] In addition, assessment of the regularity of the cone photoreceptors became possible with the use of an adaptive optic (AO) retinal imaging system, which can observe the

cone photoreceptor mosaic in near histologic resolution. The heterogeneity packing index (HPi) can serve as a sensitive biomarker for abnormalities in the regularity of the cone photoreceptors.[17,18] Several studies have reported changes in the cone mosaic in patients with diabetes.[17] Finally, the local macular visual function can be assessed reliably using microperimetry combined with fundus imaging, as this enables precise measurement as the retinal sensitivity (RS).[7,19] A previous study reported that eyes with DR had reduced RS in the area of retinal ischemia.[20]

In the current study, to gain insight into the potential association among the choroidal microcirculation and the visual function and photoreceptor structures in patients with diabetes, we conducted a prospective study and investigated the aforementioned parameters in various stages of diabetes.

Methods

Patient Recruitment

Patients with diabetes and healthy volunteers were recruited from the Department of Ophthalmology at Asahikawa Medical University Hospital between October 2018 and April 2020. The Institutional Review Board of Asahikawa Medical University approved this cross-sectional study, which adhered to the tenets of the Declaration of Helsinki. All patients provided written informed consent to participate in this research.

Study Population and Examinations

This study included consecutive patients with type 2 diabetes mellitus that fulfilled the diagnosis based on the American Diabetes Association criteria.[21] After the pupil was dilated with a drop containing tropicamide and phenylephrine hydrochloride (Santen Pharmaceutical Co., Osaka, Japan), each patient underwent a standard ophthalmic examination, including color fundus imaging using Optos 200Tx (Nikon, Tokyo, Japan), infrared fundus imaging at 30 × 30 degrees by Spectralis spectral-domain optical coherence tomography (OCT; Heidelberg Engineering GmbH, Heidelberg, Germany), spectral-domain OCT (RTVue-XR Avanti, Optovue Inc., Fremont, CA, USA), microperimetry, AO retinal imaging, and OCTA. For healthy volunteers, all examinations were performed except for AO retinal imaging.

We excluded eyes with other retinal diseases, a history of vitrectomy or laser treatment of the macula, panretinal photocoagulation (PRP) treatment within 12 weeks, antivascular endothelial growth factor (VEGF) therapy within 6 months of the study, high myopia (>6 diopters), astigmatism (>3 diopters), long axial length (>26.0 mm), significant media opacity, movement or shadow artifacts in OCTA images, or diabetic macular edema within a 3 × 3-mm macular area, which was evaluated using spectral-domain OCT.

An experienced ophthalmologist (A.S.) graded the DR images in a masked fashion based on the Early Treatment of Diabetic Retinopathy Study Severity Scale[22] and patients were divided into three groups: no diabetic retinopathy (NDR), nonproliferative diabetic retinopathy (NPDR), and proliferative diabetic retinopathy (PDR). When both eyes of a patient had the same stage of DR, the right eye was enrolled, and if the eyes had different stages of DR, the eye with the more advanced stage was included.

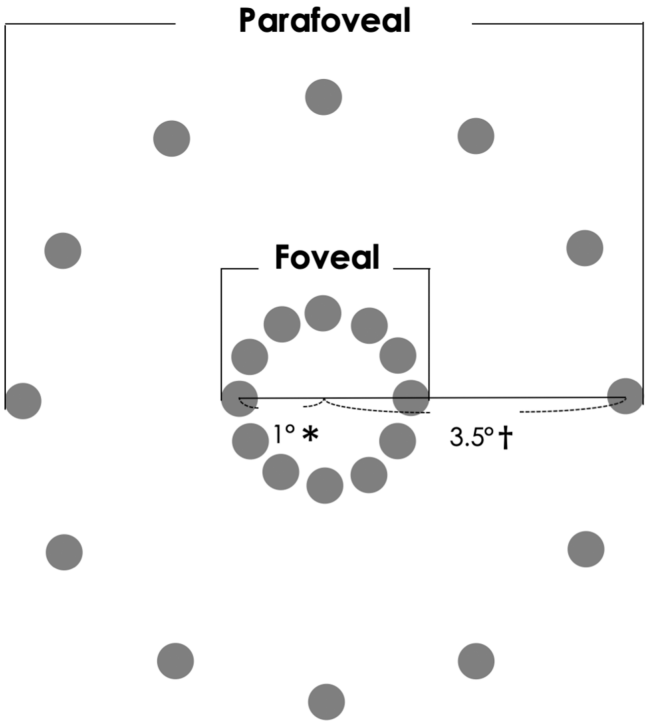

Figure 1. Evaluation pattern in microperimetry. The retinal sensitivity (RS) is measured at 24 points. The foveal and parafoveal RS values are defined as the average of the 12 points at 1 and 3.5 degrees that corresponded to 0.286 mm* and 1.001 mm† from the central fixation target, respectively.

Microperimetry

The retinal function was assessed based on the RS values obtained by microperimetry (MAIA, Centervue, Padova, Italy). Twelve points were measured at both 1 degree (foveal area) and 3.5 degrees (parafoveal area) from the central fixation target (Fig. 1). The microperimetry examination was performed in a darkened room using the following parameters: Goldman III stimuli size, a background luminance corresponding to 4asb, and the 4-2 threshold strategy.

AO Retinal Image Processing and Analysis

Cone mosaic images were acquired using the rtx1-e AO retinal flood-illumination camera (Imagine Eyes, Orsay, France). This AO camera uses infrared illumination (wavelength, 850 nm) and has a resolution of 3.5 µm, and the field of view is 4 × 4 degrees. Nine overlapping images were acquired to create a montage covering an area of 10 × 10 degrees from the central retina. The MosaicJ plugin (ImageJ, version 1.52, Image Processing and Analysis in Java; National Institutes of Health, Bethesda, MD, USA) was used to manually create a wide-field montage of the cone mosaic images[23] (Fig. 2A). At each microperimetry measurement point (Figs. 2B–D), we assessed the cone packing arrangement using Voronoi diagrams (Fig. 2F) with AOdetect software (AOdetect Mosaic XL, version 2.0 b18, Imagine Eyes) provided by the manufacturer. The algorithm successively uses Gaussian background subtraction, adaptive denoising,

Investigative Ophthalmology & Visual Science

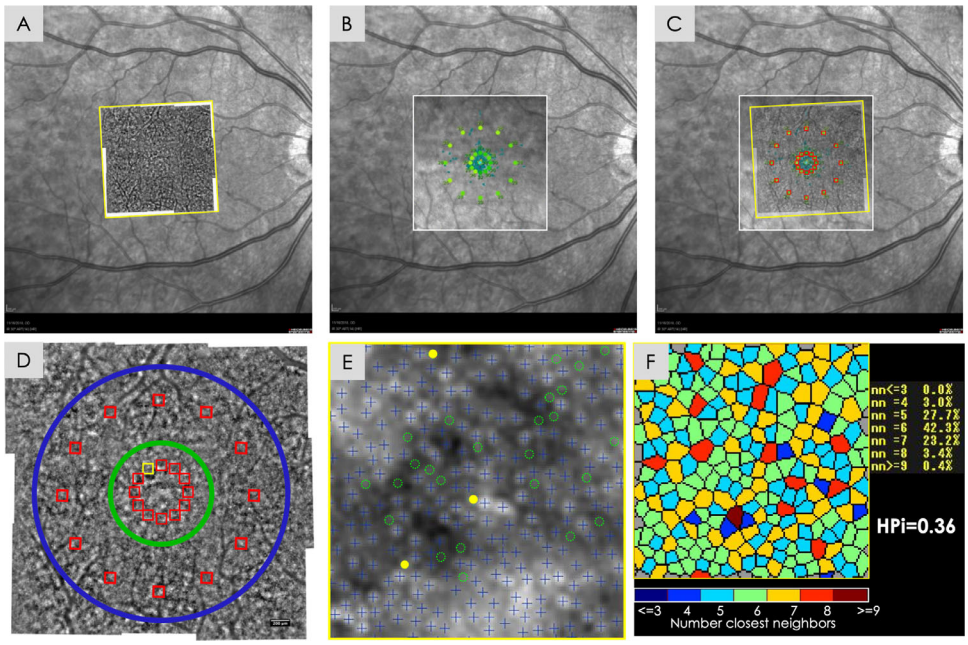

Figure 2. Analysis of cone mosaic image using AO. (**A, B**) A cone montage image and a microperimetry image are superimposed on an infrared fundus image, respectively. (**C**) The images in **A** and **B** are superimposed. (**D**) The evaluation points on a cone mosaic image. The yellow square is the sampling window for the analysis in **E**. The inner green circle indicates the foveal area, and the surrounding blue circle, which has an outer diameter of 2.5 mm and an inner diameter of 1 mm, indicates the parafoveal area in OCTA analysis. (**E**) The AOdetect software is used to analyze the cone packing arrangement. A sampling window of 0.35 × 0.35 degrees corresponds to the microperimetry spot size at the point of the microperimetry measurement. The AOdetect software recognizes and counts the cone cells automatically. Crosses indicate automatically counted cones; yellow dots, additional cones; green dashed circles; excluded cells. (**F**) A Voronoi diagram of the cone arrangement in **E**. The number of the closest neighbors (*nn*) to the cone cells (%) is determined and then the HPi is calculated using the following formula: 6-sided cell - (4-sided cell + 8-sided cell)/100.

multiscale digital filtering, and regional maxima calculation to compute estimates of the signal level and position of any small and bright round spots in the image. After this initial segmentation, the spots that fulfilled both conditions were selected: their signal was significantly higher than the photon noise, and they were not too close (i.e. <3.2 µm) to spots with a higher signal level. These conditions were intended to prevent detection of rods near cones. Once the segmentation was complete, the software analyzed the spatial distribution of the detected cells and computed several metrics, including inter-cell spacing, cell density, and the number of nearest neighbors using classical Delaunay triangulation and Voronoi tessellation algorithms. First, we chose a sampling window (Fig. 2D) of 0.35 × 0.35 degrees equal to each microperimetry spot size. Second, the AOdetect software recognized and counts the cone cells automatically (Fig. 2F). When the software missed cones, two masked graders (T.M. and T.O.) inspected and manually corrected the images after automated detection of the cone cells (Fig. 2E). According to a previous report, we analyzed only cones agreed upon by both graders and we excluded cones that were not agreed upon by both graders.[24] After the corrections, a Voronoi diagram was displayed, and cone density was calculated automatically. From each Voronoi diagram, we calculated the HPi,[17] which represents the fractional increase in four-sided and eight-sided nonhexagonal Voronoi tiles with regard to six-sided cells; a lower HPi indicates a greater deviation from the normal cone packing arrangement. All AO images were analyzed after correction for the axial length of the eye.[25]

OCTA Image Processing and Analysis

We acquired 3 × 3-mm images centered on the fovea using the RTVue-XR Avanti system (Optovue Inc., Fremont, CA, USA) with split-spectrum amplitude-decorrelation angiography software.[26] The foveal avascular zone (FAZ) parameters (i.e. FAZ area and FAZ perimeter), were calculated automatically by the built-in software (AngioVue version 2018.0.0.18). To analyze the choriocapillaris microcirculation, two sets of high-quality OCTA images were obtained from each eye (image quality, >7/10). After image acquisition, we excluded eyes with movement or shadow artifacts on the OCTA images. The retinal pigment epithelium (RPE) layer was segmented automatically by the built-in segmentation tool in the review software. The choriocapillaris slab then was segmented with a thickness of 10 µm under 31 µm from the RPE layer.[14] Thereafter, the following processing was performed using the ImageJ software. Two choriocapillaris images generated from two different OCTA cube scan sets were stacked to create a two-frame image and were registered before multiple image averaging.[27] First, the two-frame stack of superficial slabs and choriocapillaris slabs was registered, according to previous reports.[28,29] After registration, the two-frame stacks of the choriocapillaris and superficial slabs were compounded into one image by projecting the average intensity (Fig. 3A), and a central square area of 284 × 284 pixels was cropped. The averaged choriocapillaris slabs then were binarized for quantitative image analysis of the FD using the Phansalkar method (radius, 15 pixels).[14] To exclude shadows from confounding

Investigative Ophthalmology & Visual Science

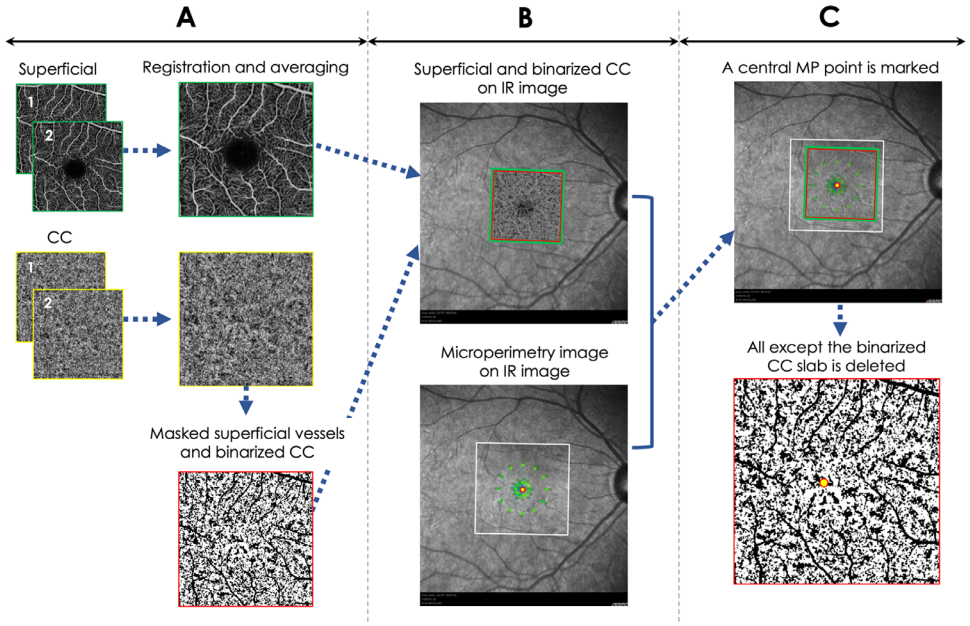

Figure 3. Analysis of FD in the choriocapillaris (CC) using OCTA. (**A**) Two superficial and choriocapillaris slabs are registered and averaged, and a central square area of 284 × 284 pixels is cropped. The averaged choriocapillaris slab is binarized using the Phansalkar method and merged with a masked image of the superficial vessels. (**B**) The averaged superficial and binarized CC slabs are superimposed on an infrared (IR) fundus image. (**C**) Two merged images in **B** are superimposed. A microperimetry (MP) central measurement point is marked on the superimposed image (yellow dot). Images other than the binarized choriocapillaris slab and the central point (yellow dot) then are deleted.

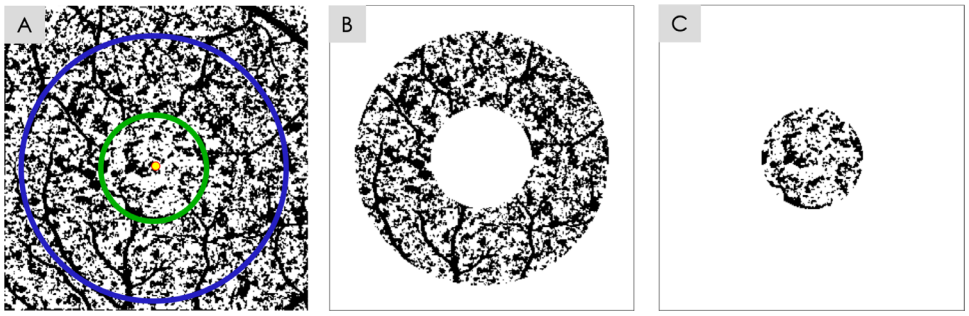

Figure 4. Foveal and parafoveal areas of FDs in a binarized choriocapillaris slab. (**A**) Circles 2.5 mm in diameter (blue circle) and 1 mm in diameter (green circle) are selected on a binarized choriocapillaris image and the central microperimetry point (yellow dot) is marked. (**B**) A 2.5-mm circle is cropped from the entire image and a 1-mm circle then is cropped from the 2.5-mm circle. The residual ring-shaped image is the parafoveal area. (**C**) The cropped 1-mm circle is the foveal area.

the analysis, a thresholded image of the large superficial retinal vessels was merged with the binarized choriocapillaris image (Fig. 3A) according to previous reports.[14,30] After binarization, a 2.5-mm-diameter circle centered on each microperimetry measurement point was cropped. A 1-mm-diameter circle image was used as the foveal area, and a ring-shaped area excluding the 1-mm central circle was used for the parafoveal area, similar to a previous study.[15] The terms "foveal" and "parafoveal" were defined, respectively, by the area of the center and the area of the inner circle in the Early Treatment Diabetic Retinopathy Study (ETDRS) grid. The parafoveal area of the ETDRS grid generally is donut-shaped with an outer diameter of 3 mm and an inner diameter of 1 mm. However, the outer diameter of 2.5 mm was used in the current study to prevent the boundary edge of the OCTA images from being included in the selected area of analysis. The ratio of black pixels in the area, except for the superficial blood vessels, was calculated as the FD (%) (Fig. 4). All OCTA parameters were analyzed after correction for the axial length of the eye.[31]

Image Overlay

Using the retinal vasculature as a guide, the AO montage image, a microperimetry image, and OCTA images then were overlaid manually over the infrared fundus images to facilitate correlations among the RS, HPi, and FD, respectively (Figs. 2, 3B, 3C). Twelve cone mosaic and microperimetry measurement points were arranged within each 1-mm-diameter central area and the 2.5-mm donut-shaped area. The averaged values of the HPi and RS within these areas were defined similarly to the OCTA analysis areas of FD, that is, as foveal and parafoveal (Fig. 2D). These processes were

Table. Patient Characteristics

Parameter	Control ($n = 13$)	NDR ($n = 4$)	NPDR ($n = 12$)	PDR ($n = 10$)	*P* Value
Age, mean ± SD, years	53.2 ± 9.1	53.8 ± 9.2	62.5 ± 8.2	49.7 ± 13.3	0.033*
Sex					0.82
Men, *n*	7	2	7	5	1
Women, *n*	6	2	5	5	
Hemoglobin A1c, mean ± SD, %	–	6.6 ± 0.7	6.9 ± 0.9	7.2 ± 1.6	0.7
Duration, mean ± SD, years	–	7.5 ± 7.7	13.5 ± 7.2	12.6 ± 10.5	0.54
PRP, *n*	–	0	5	10	<0.001†
Anti-VEGF therapy	–	0	1	1	1
Best-corrected logMAR VA, mean ± SD	−0.07 ± 0.02	−0.08 ± 0.0	−0.03 ± 0.09	−0.03 ± −0.1	0.3
Lens status					0.13
Phakia, *n*	13	3	9	7	
Pseudophakia, *n*	0	1	3	3	
CRT, mean ± SD, µm	252 ± 19	261 ± 44	258 ± 24	267 ± 23	0.53
FAZ materials					
FAZ area in inner retina, mean ± SD, mm^2	0.30 ± 0.07	0.34 ± 0.1	0.38 ± 0.12	0.33 ± 0.1	0.23
FAZ perimeter in inner retina, mean ± SD, mm	2.2 ± 0.29	2.3 ± 0.41	2.5 ± 0.39	2.5 ± 0.44	0.26
Central area cone density, mean ± SD, cone/mm^2	–	26,924 ± 4,359	21,848 ± 2,733	20,210 ± 3,450	0.044‡

*One-way analysis of variance (post hoc Holm test); NPDR < PDR ($P < 0.05$).
† Fisher's exact test (post hoc Holm test); NDR < NPDR($P < 0.01$), NPDR < PDR ($P < 0.05$).
‡ One-way analysis of variance (post hoc Holm test); NDR > PDR ($P < 0.05$).
HbA1c, hemoglobin A1c; logMAR VA, logarithm of the minimum angle of resolution visual acuity; CRT, central retinal thickness.

performed by GNU Image Manipulation Program (version 2.10.10, GIMP Development Team).

Statistical Analysis

To obtain the foveal and parafoveal RS and HPi values, we calculated the average of 12 points within the foveal and parafoveal areas. The categorical values were compared using Fisher's exact test. One-way analysis of variance was performed to compare the FD, RS, and HPi among the eyes with NDR, NPDR, and PDR at the foveal and parafoveal areas using the Holm post hoc test. The relationships between the FD and HPi and between the FD and RS were determined with Pearson correlation coefficients at the foveal and parafoveal areas. Statistical analyses were performed using EZR[32] (Jichi Medical University Saitama Medical Center), a graphic user interface for R (The R Foundation for Statistical Computing, version 3.6.0), and a modified version of the R commander (version 2.5-3). All measurements are expressed as the means ± standard errors. All *P* values were based on two-sided tests; $P < 0.05$ was considered statistically significant.

Results

Thirteen healthy participants and 26 patients with diabetes were recruited for this study, 4 patients with NDR, 12 with NPDR, and 10 with PDR. Patients with NPDR were significantly ($P = 0.033$) older than the PDR group, and a significantly ($P = 0.034$) increased number of patients had a history of PRP to treat advanced DR. Other parameters, including the FAZ area and FAZ perimeter in the inner retina, did not differ significantly. The cone density in the foveal area was significantly ($P = 0.044$) decreased in patients with PDR compared to patients with NDR ($P = 0.043$; Table).

At both the foveal and parafoveal areas, the FD was significantly ($P = 0.003$ and $P = 0.006$, respectively) higher in eyes with PDR than in the control eyes ($P = 0.001$ and $P = 0.005$, respectively), and the FD increased numerically with advanced DR, although the difference did not reach significance. The parafoveal FD was significantly ($P < 0.001$) higher than the foveal FD only in patients with NPDR (Fig. 5A). Overall, the RS decreased with advanced disease stage. The foveal and parafoveal RS values in NPDR and PDR were significantly lower compared with the control and NDR values. The foveal RS was significantly ($P = 0.033$) lower than the parafoveal RS in patients with PDR. The HPi, especially at the parafoveal area, was decreased significantly in those with DR (i.e. NPDR and PDR) compared to those with NDR ($P = 0.012$ and $P = 0.037$, respectively), but there was no difference between NPDR and PDR. There also were no differences in the foveal HPi values among all groups. The foveal HPi was significantly ($P = 0.049$) lower than the parafoveal HPi in patients with NDR (Fig. 6).

No association was seen between the RS and FD in NDR; however, a significant correlation was found between the FD and RS in patients with NPDR and PDR both at the foveal and parafoveal areas (fovea, $r = -0.58$; $P = 0.046$ and $r = -0.82$; $P = 0.003$; parafovea, $r = -0.59$; $P = 0.044$ and $r = -0.72$; and $P = 0.019$; Figs. 7A–F). There was no significant correlation between the FD and RS in the controls (foveal, $r = 0.05$; $P = 0.87$, parafoveal, $r = -0.22$; $P = 0.47$). The OCTA parameters for retinal circulation, including the FAZ area and FAZ perimeter in the inner retina, did not differ. In contrast, the association between the HPi and FD was poor. In both the foveal and parafoveal areas, there was no significant correlation between the FD and HPi in any group (Figs. 8A–F).

Discussion

In the current study, the foveal and parafoveal FD were increased significantly in patients with PDR compared with the control participants. The current study corroborates the results of a previous study that reported that the capillary loss in the choriocapillaris tended to increase in advanced DR.[11] However, in contrast to a previous study,[5] the parafoveal choriocapillaris microcirculation did

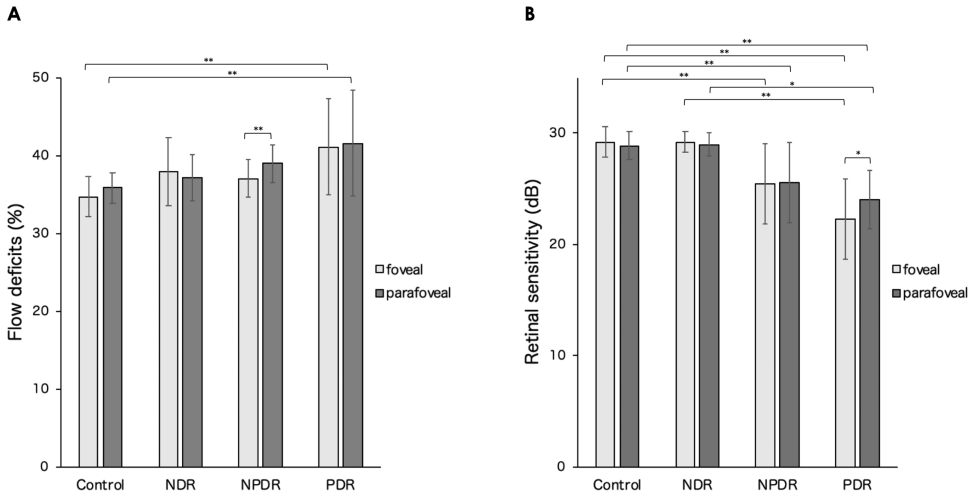

Figure 5. Each parameter of the foveal and parafoveal areas in each group of control and patients with DR. (**A**) The FD values. (**B**) The RS values. Statistical analyses between the areas and among the patients with DR were performed using the paired *t*-test and one-way analysis of variance with post hoc (Holm test), respectively. The mean value ± SD is indicated for each group. $^{*}P < 0.05$, $^{**}P < 0.01$. dB, decibels.

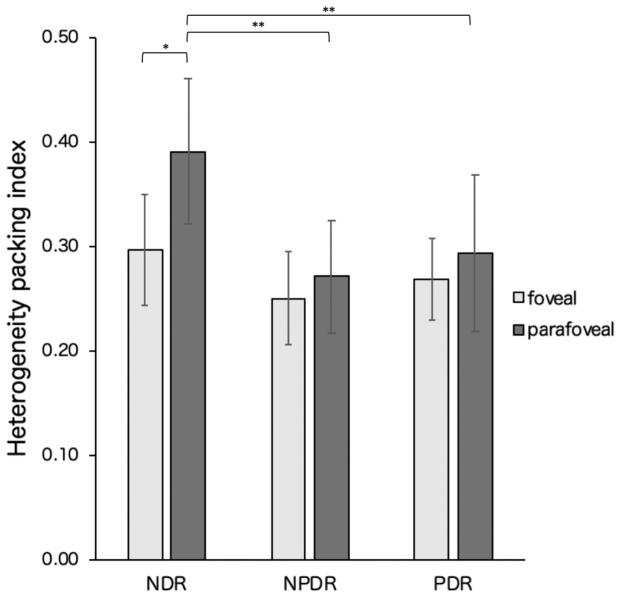

Figure 6. The HPi values of the foveal and parafoveal areas in each group of patients with DR. Statistical analyses between the areas and among the patients with DR were performed using the paired *t*-test and one-way analysis of variance with post hoc (Holm test), respectively. The mean value ± SD is indicated for each group. $^{*}P < 0.05$, $^{**}P < 0.01$. dB, decibels.

not differ significantly across all diabetes mellitus groups, suggesting that the parafoveal choriocapillaris microcirculation may not depend on DR progression.

Regarding the FD, there was no significant difference between NDR and NPDR in the foveal area. Analysis of the choriocapillaris FD may be affected by several factors. In addition to DR severity, DR treatment may affect the choriocapillaris. Anti-VEGF therapy can decrease the choriocapillaris capillary density.[33] In contrast, PRP reportedly increases the choriocapillaris microcirculation at the foveal area in patients with severe NPDR and PDR, as shown by laser Doppler flowmetry.[34] Because some current patients with NPDR had a medical history of PRP and injection of anti-VEGF therapy, the most plausible explanation for the absence of a difference in the FD between NDR and NPDR is that the FD in these patients was confounded by treatments.

The current study identified significant differences in the RS among control and all DR groups in the foveal and parafoveal areas, and the RS tended to decrease in advanced DR. Consistent with our results, several studies in which the MP-1 microperimeter (Nidek, Aichi, Japan) was used reported that the foveal and parafoveal RS values were associated with progression of DR.[35,36] In addition, compared with the parafoveal RS, the foveal RS was reduced in patients with PDR in the current study. A previous study reported that the severity of foveal ischemia was related to outer retinal damage[37]; notably eyes with PDR are prone to develop foveal ischemia.[38]

Although the foveal HPi did not differ significantly across all groups, the parafoveal HPi in patients with NPDR and PDR was significantly lower than that of NDR, suggesting that the parafoveal but not the foveal cone regularity may decrease as the DR developments. In patients with NDR, a previous study found that the thickness of the foveal photoreceptor layer decreased significantly compared with the control.[39] Regarding a regional difference, a previous report showed that the foveal cone regularity was higher than the parafoveal cone regularity in normal subjects.[40] In contrast, the current study identified a significant difference in the cone regularity between the foveal and parafoveal areas in patients with NDR; the foveal cone mosaic may be more irregular in patients with NDR compared to the parafoveal cone mosaic. Moreover, a previous study using AO-scanning laser ophthalmoscopy indicated that parafoveal cone regularity decreased in DR,[41] which was consistent with our result. Therefore, early changes in the cone mosaic in diabetic eyes might be detected at the foveal area. However, regarding the cone measurements, a previous study reported that cone reflectivity fluctuates and there are cones with low reflectivity even in normal eyes.[42] In the current study, the automated analysis software often missed those cones with low reflectivity. However, those missed cones were unclear and difficult to correct completely

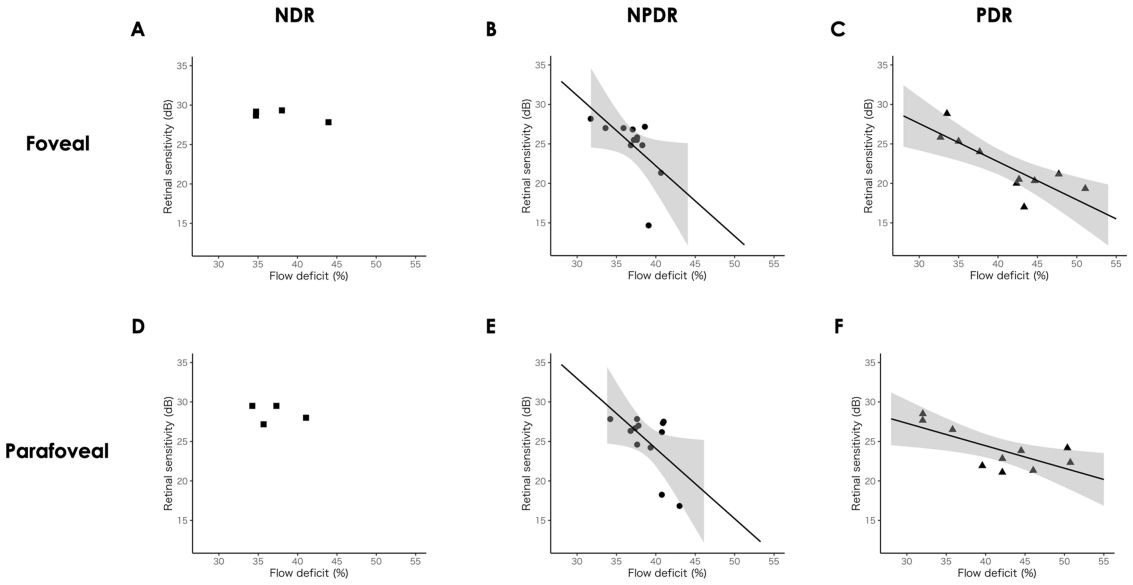

Figure 7. The FD and RS values in patients with diabetes. There is no significant correlation (**A, D**) in NDR, but there are significant differences (**B, E**) in NPDR (fovea; $r = -0.58$, $P = 0.046$; parafovea; $r = -0.59$, $P = 0.044$) and (**C, F**) in PDR (fovea; $r = -0.82$, $P = 0.003$; parafovea; $r = -0.72$, $P = 0.019$). dB, decibels.

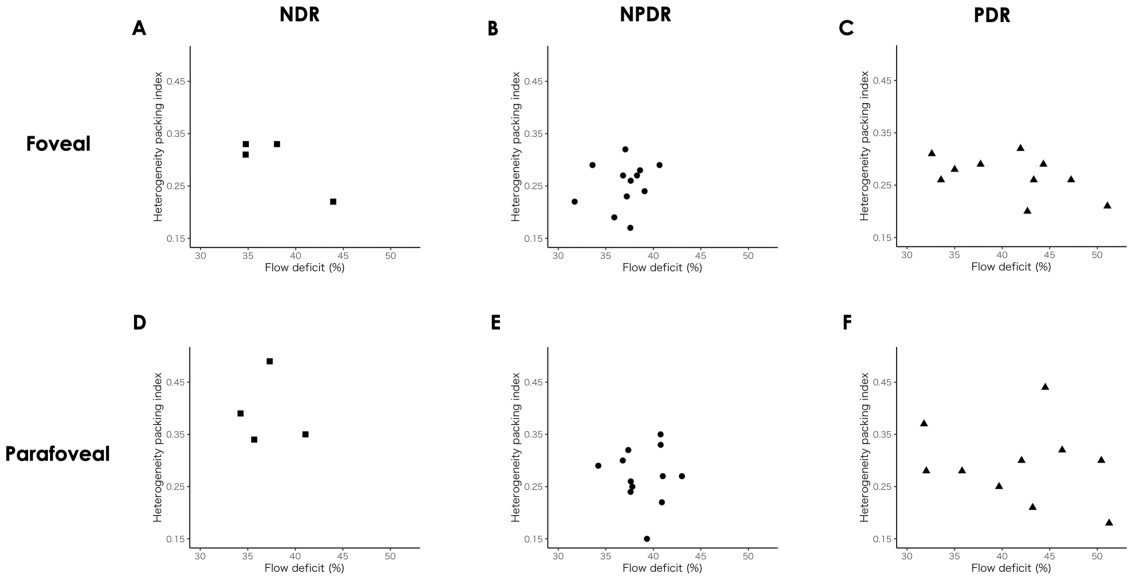

Figure 8. The association between the FD and HPi in patients with diabetes. In the foveal area, there is no significant correlation (**A–C**) in all groups. In the parafoveal area, the FD is not correlated significantly with the HPi (**D–F**) across all groups.

manually from the area of low reflectivity in addition to the automatically selected cones. Therefore, we corrected only "the clearly detected cells" by two graders. Those might affect the cone measurements and lead to underestimation of the cone density. Therefore, the HPi values might be affected by this limitation of the current study. Regarding the region at 3.5 degrees, there are many rods surrounding the cone,[43] and a cluster of neighboring rods can blur together and look like a single cone, because the rtx1 only has a resolution of up to 3.5 µm possibly causing overestimations of the numbers of cones in the periphery. The cone density and HPi values may have been affected by these limitations.

The current study found a significant correlation between the choriocapillaris microcirculation and RS, irrespective of the area evaluated in the NPDR and PDR groups, but not in the control and NDR groups, suggesting that visual dysfunction is associated with choriocapillaris ischemia in eyes with DR. Experimentally, rat photoreceptors are specifically vulnerable to hypoxia.[44] A clinical study also indicated that loss of the choriocapillaris was related to the functional visual impairment in DR.[11] In conditions in which retinal homeostasis is impaired by development and progression of DR,[45,46] photoreceptor function may be highly vulnerable to changes in the choroidal circulation in eyes

with NPDR and PDR. We speculated that choriocapillaris ischemia contributes to visual dysfunction through photoreceptor malfunction in eyes with DR. We suspect that the RS measured with the current protocol may not be sufficiently sensitive to evaluate minute changes in eyes with NDR, because there was almost no difference in the RS between the control and NDR groups.

No correlation was found between the choriocapillaris microcirculation and cone regularity in both areas of NPDR and PDR despite an association between the choriocapillaris microcirculation and RS, suggesting that the effect of choriocapillaris flow may differ between the RS and cone mosaic. The structural damage to the cone photoreceptors in eyes with DR persists over time[47]; cumulative damage resulting from a long-term abnormality of the choroidal microcirculation may result in irreversible changes in the cone mosaic in DR. However, the RS is dynamic and reversible (e.g. it improves after anti-VEGF treatment of macular edema).[48,49] Therefore, we believe it is rational to assume that the changes in the cone mosaic may not necessarily depend on the choriocapillaris microcirculation at the time of the examination.

This study had several limitations. The study sample size was relatively small and the study design was cross-sectional. We were unable to determine causality. The HPi might be affected by the resolution of the rtx1 instrument. In addition, patients with NPDR were older than in the PDR group. The age difference may have affected our results, although a previous report did not show an association between reduced choriocapillaris flow and age in patients with DR.[5] Many patients had undergone previous treatments either of anti-VEGF therapy or PRP. Larger-scale studies matching the effects of confounding factors affecting the chorioretinal blood flow, such as drugs[50] and systemic parameters,[51] are needed to confirm our findings. Even in NDR eyes, the range of FD varied, and some eyes had more than 40% both in the foveal and parafoveal areas. It may be helpful to follow the eyes with NDR and NPDR in a future longitudinal study to observe if the FD in the choriocapillaris predicts the worsening or progression of DR.

In summary, the current study identified an association between changes in the choriocapillaris microcirculation and the RS and cone photoreceptor mosaic in patients with diabetes. We found that changes in the choriocapillaris microcirculation are associated with visual function in eyes with DR. We believe these findings provide valuable insight into the pathophysiology of functional impairment and structural damage in patients with diabetes.

Acknowledgments

The authors thank Nicolas Chateau, PhD (Imagine Eyes, Orsay, France) for providing the AOdetect software.

Disclosure: **T. Ro-Mase,** None; **S. Ishiko,** None; **T. Omae,** None; **A. Ishibazawa,** None; **A. Shimouchi,** None; **A. Yoshida,** None

References

1. Romero-Aroca P. Managing diabetic macular edema: the leading cause of diabetes blindness. *World J Diabetes*. 2011;2:98–104.
2. Birol G, Wang S, Budzynski E, Wangsa-Wirawan ND, Linsenmeier RA. Oxygen distribution and consumption in the macaque retina. *Am J Physiol Circ Physiol*. 2007;293:H1696–H1704.
3. Wangsa-Wirawan ND, Linsenmeier RA. Retinal oxygen: fundamental and clinical aspects. *Arch Ophthalmol*. 2003;121:547–557.
4. Lutty GA, Cao J, McLeod DS. Relationship of polymorphonuclear leukocytes to capillary dropout in the human diabetic choroid. *Am J Pathol*. 1997;151:707–714.
5. Dodo Y, Suzuma K, Ishihara K, et al. Clinical relevance of reduced decorrelation signals in the diabetic inner choroid on optical coherence tomography angiography. *Sci Rep*. 2017;7:5227.
6. Spaide RF, Curcio CA. Anatomical correlates to the bands seen in the outer retina by optical coherence tomography: literature review and model. *Retina*. 2011;31:1609.
7. Unoki N, Nishijima K, Sakamoto A, et al. Retinal sensitivity loss and structural disturbance in areas of capillary nonperfusion of eyes with diabetic retinopathy. *Am J Ophthalmol*. 2007;144:755–760.e1.
8. Wakazono T, Ooto S, Hangai M, Yoshimura N. Photoreceptor outer segment abnormalities and retinal sensitivity in acute zonal occult outer retinopathy. *Retina*. 2013;33:642–648.
9. Agemy SA, Scripsema NK, Shah CM, et al. Retinal vascular perfusion density mapping using optical coherence tomography angiography in normals and diabetic retinopathy patients. *Retina*. 2015;35:2353–2363.
10. Nesper PL, Roberts PK, Onishi AC, et al. Quantifying microvascular abnormalities with increasing severity of diabetic retinopathy using optical coherence tomography angiography. *Invest Ophthalmol Vis Sci*. 2017;58:Bio307–bio315.
11. Conti FF, Qin VL, Rodrigues EB, et al. Choriocapillaris and retinal vascular plexus density of diabetic eyes using split-spectrum amplitude decorrelation spectral-domain optical coherence tomography angiography. *Br J Ophthalmol*. 2019;103:452–456.
12. Li L, Almansoob S, Zhang P, Zhou YD, Tan Y, Gao L. Quantitative analysis of retinal and choroid capillary ischaemia using optical coherence tomography angiography in type 2 diabetes. *Acta Ophthalmol*. 2019;97:240–246.
13. Yang J, Wang E, Zhao X, et al. Optical coherence tomography angiography analysis of the choriocapillary layer in treatment-naive diabetic eyes. *Graefes Arch Clin Exp Ophthalmol*. 2019;257:1393–1399.
14. Spaide RF. Choriocapillaris flow features follow a power law distribution: implications for characterization and mechanisms of disease progression. *Am J Ophthalmol*. 2016;170:58–67.
15. Zheng F, Zhang Q, Shi Y, et al. Age-dependent changes in the macular choriocapillaris of normal eyes imaged with swept-source optical coherence tomography angiography. *Am J Ophthalmol*. 2019;200:110–122.
16. Choi W, Mohler KJ, Potsaid B, et al. Choriocapillaris and choroidal microvasculature imaging with ultrahigh speed OCT angiography. *PLoS One*. 2013;8:e81499.
17. Lombardo M, Parravano M, Serrao S, Ziccardi L, Giannini D, Lombardo G. Investigation of Adaptive optics imaging biomarkers for detecting pathological changes of the cone mosaic in patients with type 1 diabetes mellitus. *PLoS One*. 2016;11:e0151380.
18. Nesper PL, Scarinci F, Fawzi AA. Adaptive optics reveals photoreceptor abnormalities in diabetic macular ischemia. *PLoS One*. 2017;12:e0169926.
19. Parodi MB, Triolo G, Morales M, et al. MP1 and Maia fundus perimetry in healthy subjects and patients affected by retinal dystrophies. *Retina*. 2015;35:1662–1669.

20. Yu S, Wang F, Pang CE, Yannuzzi LA, Freund KB. Multimodal imaging findings in retinal deep capillary ischemia. *Retina*. 2014;34:636–646.
21. American Diabetes A. Standards of medical care in diabetes–2014. *Diabetes Care*. 2014;37(Suppl 1):S14–S80.
22. Group ETDRSR. Grading diabetic retinopathy from stereoscopic color fundus photographs—an extension of the modified Airlie House classification: ETDRS report number 10. *Ophthalmology*. 1991;98:786–806.
23. Bukowska DM, Wan SL, Chew AL, et al. Fundus autofluorescence in rubella retinopathy: correlation with photoreceptor structure and function. *Retina*. 2017;37:124–134.
24. Soliman MK, Sadiq MA, Agarwal A, et al. High-resolution imaging of parafoveal cones in different stages of diabetic retinopathy using adaptive optics fundus camera. *PLoS One*. 2016;11:e0152788.
25. Bennett AG, Rudnicka AR, Edgar DF. Improvements on Littmann's method of determining the size of retinal features by fundus photography. *Graefe's Arch Clin Exp Ophthalmol*. 1994;232:361–367.
26. Jia Y, Tan O, Tokayer J, et al. Split-spectrum amplitude-decorrelation angiography with optical coherence tomography. *Opt Express*. 2012;20:4710–4725.
27. Borrelli E, Shi Y, Uji A, et al. Topographic analysis of the choriocapillaris in intermediate age-related macular degeneration. *Am J Ophthalmol*. 2018;196:34–43.
28. Uji A, Balasubramanian S, Lei J, Baghdasaryan E, Al-Sheikh M, Sadda SR. Impact of multiple en face image averaging on quantitative assessment from optical coherence tomography angiography images. *Ophthalmology*. 2017;124:944–952.
29. Uji A, Balasubramanian S, Lei J, Baghdasaryan E, Al-Sheikh M, Sadda SR. Choriocapillaris imaging using multiple en face optical coherence tomography angiography image averaging. *JAMA Ophthalmol*. 2017;135:1197–1204.
30. Sacconi R, Borrelli E, Corbelli E, et al. Quantitative changes in the ageing choriocapillaris as measured by swept source optical coherence tomography angiography. *Br J Ophthalmol*. 2019;103:1320–1326.
31. Sampson DM, Gong P, An D, et al. Axial length variation impacts on superficial retinal vessel density and foveal avascular zone area measurements using optical coherence tomography angiography. *Invest Ophthalmol Vis Sci*. 2017;58:3065–3072.
32. Kanda Y. Investigation of the freely available easy-to-use software "EZR" for medical statistics. *Bone Marrow Transpl*. 2013;48:452–458.
33. Hikichi T, Agarie M. Reduced vessel density of the choriocapillaris during anti-vascular endothelial growth factor therapy for neovascular age-related macular degeneration. *Invest Ophthalmol Vis Sci*. 2019;60:1088–1095.
34. Takahashi A, Nagaoka T, Sato E, Yoshida A. Effect of panretinal photocoagulation on choroidal circulation in the foveal region in patients with severe diabetic retinopathy. *Br J Ophthalmol*. 2008;92:1369–1373.
35. Nittala MG, Gella L, Raman R, Sharma T. Measuring retinal sensitivity with the microperimeter in patients with diabetes. *Retina*. 2012;32:1302–1309.
36. Gella L, Raman R, Kulothungan V, Saumya Pal S, Ganesan S, Sharma T. Retinal sensitivity in subjects with type 2 diabetes mellitus: Sankara Nethralaya Diabetic Retinopathy Epidemiology and Molecular Genetics Study (SN-DREAMS II, Report No. 4). *Br J Ophthalmol*. 2016;100:808–813.
37. Yalçın NG, Ş Özdek. The relationship between macular cyst formation and ischemia in diabetic macular edema. *Turkish J Ophthalmol*. 2019;49:194–200.
38. Sim DA, Keane PA, Zarranz-Ventura J, et al. The effects of macular ischemia on visual acuity in diabetic retinopathy. *Invest Ophthalmol Vis Sci*. 2013;54:2353–2360.
39. Verma A, Rani PK, Raman R, et al. Is neuronal dysfunction an early sign of diabetic retinopathy? Microperimetry and spectral domain optical coherence tomography (SD-OCT) study in individuals with diabetes, but no diabetic retinopathy. *Eye*. 2009;23:1824–1830.
40. Park SP, Chung JK, Greenstein V, Tsang SH, Chang S. A study of factors affecting the human cone photoreceptor density measured by adaptive optics scanning laser ophthalmoscope. *Exp Eye Res*. 2013;108:1–9.
41. Lammer J, Prager SG, Cheney MC, et al. Cone photoreceptor irregularity on adaptive optics scanning laser ophthalmoscopy correlates with severity of diabetic retinopathy and macular edema. *Invest Ophthalmol Vis Sci*. 2016;57:6624–6632.
42. Pallikaris A, Williams DR, Hofer H. The reflectance of single cones in the living human eye. *Invest Ophthalmol Vis Sci*. 2003;44:4580–4592.
43. Curcio CA, Sloan KR, Kalina RE, Hendrickson AE. Human photoreceptor topography. *J Comp Neurol*. 1990;292:497–523.
44. Wellard J, Lee D, Valter K, Stone J. Photoreceptors in the rat retina are specifically vulnerable to both hypoxia and hyperoxia. *Vis Neurosci*. 2005;22:501–507.
45. Omri S, Behar-Cohen F, de Kozak Y, et al. Microglia/macrophages migrate through retinal epithelium barrier by a transcellular route in diabetic retinopathy: role of PKCζ in the Goto Kakizaki rat model. *Am J Pathol*. 2011;179:942–953.
46. Pannicke T, Iandiev I, Wurm A, et al. Diabetes alters osmotic swelling characteristics and membrane conductance of glial cells in rat retina. *Diabetes*. 2006;55:633–639.
47. Sawides L, Sapoznik KA, de Castro A, et al. Alterations to the foveal cone mosaic of diabetic patients. *Invest Ophthalmol Vis Sci*. 2017;58:3395–3403.
48. Mylonas G, Sacu S, Dunavoelgyi R, et al. Response of retinal sensitivity to ranibizumab treatment of macular edema after acute branch retinal vein occlusion. *Retina*. 2013;33:1220–1226.
49. Vujosevic S, Berton M, Bini S, Casciano M, Cavarzeran F, Midena E. Hyperreflective retinal spots and visual function after anti-vascular endothelial growth factor treatment in center-involving diabetic macular edema. *Retina*. 2016;36:1298–1308.
50. Nagaoka T, Takahashi A, Sato E, et al. Effect of systemic administration of simvastatin on retinal circulation. *Arch Ophthalmol*. 2006;124:665–670.
51. Nagaoka T, Yoshida A. Relationship between retinal blood flow and renal function in patients with type 2 diabetes and chronic kidney disease. *Diabetes Care*. 2013;36:957–961.

Investigative Ophthalmology & Visual Science